

Heterogeneous Catalytic Ozonation of Acid blue 62 Over Nanorod Fe-OMS-2

Tuyet-Mai Tran-Thuy*, Hoa-Hung Lam, Quoc-Tuan Dang, Thuy-Sang Phan, Duc-Nguyen Truong-Pham, Dung Van Nguyen, Trung Dang-Bao

Faculty of Chemical Engineering, Ho Chi Minh City University of Technology, VNU-HCM, 268 Ly Thuong Kiet, District 10, Ho Chi Minh City, Vietnam
 tuyetmai@hcmut.edu.vn

In this work, nanorod materials prepared by refluxed method (K-OMS-2) and by co-precipitation method (Fe-OMS-2) were analyzed by X-ray diffraction (XRD), Raman spectroscopy and scanning electron microscopy (SEM). Non-catalytic and heterogeneous catalytic ozonation processes of acid blue 62 (AB-62) were tested under the bubbling O_3 /air flow, at room temperature (RT). Comparing to ozonation over Fe-OMS-2, both adsorption and non-catalytic ozonation of AB-62 showed much lower removal efficiency. These results evidenced a positive role of nanorod Fe-OMS-2 in removal of ~80% of AB-62 after 50 min of O_3 bubbling. The pseudo first-order reaction with respect to the AB-62 was observed from ozonation over K-OMS-2 and Fe-OMS-2 catalysts. The reaction rate measured from Fe-OMS-2 is three times faster than that from K-OMS-2 probably contributed from a synergistic effect between O_3 and defects on the surface of Fe-OMS-2.

1. Introduction

Removal of dye effluents has much more attracted because of a huge industrial wastewater from the development of textile manufactures. Many methods have been applied to decolorize dye wastewater like settling methods, physical chemical processes (using inhibit flocculations, coagulants, adsorbents), biological method (Wang et al., 2018), oxidation in homogeneous and over heterogeneous catalyses, even advanced oxidations with the assistance of H_2O_2 (He, 2018) or ozone (O_3) in the presence (Wu et al., 2008) and in the absence of catalysts- non catalytic ozonation- for removal of orange 16 (Turhan and Ozturkcan 2013) or for the treatment of agro industrial wastewaters (Martins and Quinta-Ferreira, 2014). Among those, heterogeneous catalytic ozonation that can work well at neutral pH promises a great application for dye wastewater treatment (Zhao et al., 2009) or directly ozonation of phenolic compounds over perovskite (Martins and Quinta-Ferreira, 2014). It was commonly reported that ozonation of dye organic compounds showed a good activity in harsh pH ranges. For instance, ozonation of 1,3,6-naphthalenetrisulphonic acid over commercial carbon was noticeably promoted at pH 2-3 (Rivera-Utrilla and Sanchez-Polo, 2002). Removal of methylene blue (MB) on acid-treated zeolite was reported better efficiency at pH 10 with ozone (Valdés et al., 2012). Other reported that 100% of MB solution at pH 2 was ozonized on TiO_2 / active carbon (Zhang et al., 2009). In addition, Fe-based heterogeneous catalyst like $CoFe_2O_4$ was reported an excellent activity in ozonation of melanoidin (Oliveira et al., 2019); binary oxide of Fe-Si (Yuan et al., 2018) was also considered as important catalyst in ozonation of 4-chloronitrobenzene; nanoparticle $BiFeO_3$ was reported with high activity in photocatalytic ozonation of norfloxacin (Yin et al., 2016). Cryptomelane structure (K-OMS-2, K^+ cations and H_2O dominated in the tunnels constituted by octahedral unit of MnO_6) was reported as good and convenient catalyst for oxidation. Additionally, metal-doped cryptomelane like Co-doped OMS-2 was reported as water-tolerant catalyst for CO oxidation (Yang et al., 2017), or Fe doping enhanced significant O_3 oxidation in dry condition (Jia et al., 2017). However, the Fe-OMS-2 catalyst activity decayed remarkably with time at high relative humidity (Jia et al., 2017) indicating that surrounding humidity considerably affected on O_3 decomposition over Fe-OMS-2. Interestingly, Yuan et al., reported that a prohibition of O_3 decomposition process was proposed as a crucial step to provoke active $\cdot OH$ species at the Fe-Si interface for ozonation of chloronitrobenzene in aqueous solution (Yuan et al., 2018). This indicates that aqueous medium may preclude

O₃ decomposition forward O₂, but provoke the long-life of OH radical over Fe-OMS-2 - one of the strongest oxidants known. In this work, cryptomelane materials of OMS-2 and Fe-OMS-2 will be prepared and the effect of *OH species on the surface of Fe-OMS-2 on catalytic performance in ozonation of AB-62 at room temperature, neutral pH value will be interpreted. Furthermore, a synergistic effect between *OH species/Fe-OMS-2 and O₃ that may accelerate catalyst activity will be reported.

2. Materials and methods

All materials from Shanghai Chemical Reagent, Inc. were analytical grade, used as received without further purification. KMnO₄ solution was added into MnSO₄ solution while concentrated HNO₃ was used to adjust pH < 2. The mixture was then refluxed at 100 °C for 24 h. After filtering, washing and drying at 120 °C overnight, K-OMS-2 material was collected. Fe-OMS-2 was prepared by co-precipitation of Fe³⁺ cation in the solution of Mn⁷⁺ and Mn³⁺ cations such that the molar concentration of Fe³⁺ is 0.1 M in the final mixture (DeGuzman et al., 1994). X-ray powder diffraction (XRD) was performed using a Brucker AXS D8 diffractometer over the 2θ range of 10-90 ° and the scan rate was of 1°/min (Zhao et al., 2019). Scanning Electron Microscope (SEM) images were recorded with a (FE-SEM) S-4800, and an accelerating voltage of 10 kV. Powder samples were adhered on carbon tape, then underwent Pt sputter coating. Raman spectra were collected on a UniRAM micro-Raman spectrometer with laser excitation (λ = 532 nm). Water adsorption measurement (only for the Raman shift testing) were examined by following steps: about 0.1 g of solid sample put in a glass U tube would be degassed in N₂ flow at 200 °C for 6 h. Then, H₂O vapour in N₂ flow was introduced to the tube at 27 °C for adsorption. The tube was weighted with time until getting a stable value for saturated adsorption. A flow of 0.5 L/min of air contained 58 μmol/min of O₃ (checked with a titration method (Rakness et al., 1996) was designed for ozonation of AB-62. Typically, O₃ (produced from clean air by use of Vina Ozone Generator model VN3 with Cold Plasma Technology) mixed with air was bubbled in the reaction batch of 0.5 L of AB-62 with a desired catalyst amount, pH 7, at 27 °C (RT). The gas coming out was connected to KI solution before exhausting outside. Small amount of liquid effluent will be withdrawn by a glass syringe versus time. After centrifugal force, liquid effluent was diluted and measured absorbance index at wavelength of 637 nm by a UV-Vis spectroscopy. To test the durability of catalyst, Fe-OMS-2 after ozonation was washed, dried at 120 °C overnight and would be used for further catalyst activity testing.

3. Results and discussion

3.1 Results

The XRD patterns of K-OMS-2 and Fe-OMS-2 show typical diffraction peak positions at 2θ of 12.8 °; 18 °; 28.8 °; 37.3 °; 49.9 ° and 58.3 ° in Figure 1a. Those peaks were assigned for cryptomelane structure (JPCDS 291020) confirming the presence of K-OMS-2 and Fe-OMS-2 (Duan et al., 1995; Villegas et al., 2005). Raman spectroscopy of K-OMS-2, Fe-OMS-2 before and after water adsorption is shown in Figure 1b.

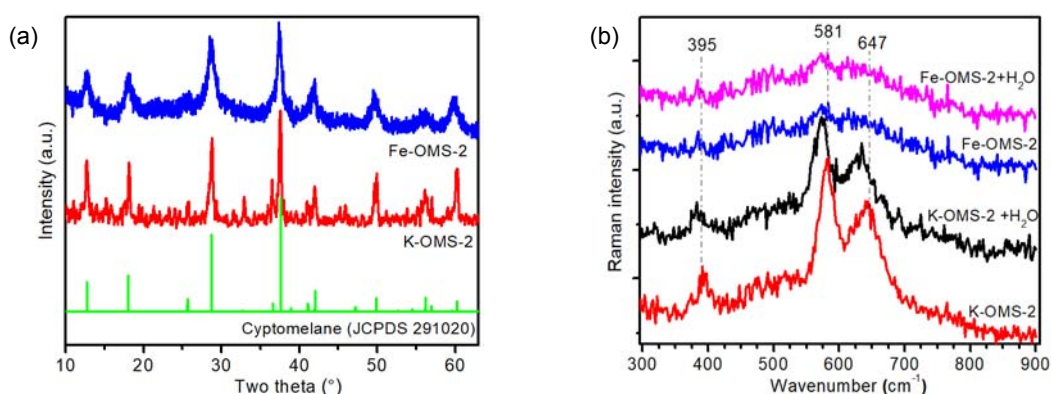


Figure 1: XRD patterns of (a) K-OMS-2 and Fe-OMS-2 and Raman spectroscopy of (b) K-OMS-2 and Fe-OMS-2 before and after H₂O adsorption (K-OMS-2 + H₂O; Fe-OMS-2 + H₂O).

The Raman spectrum of K-OMS-2 contains three bands at 395, 581, 641 cm⁻¹ revealing a well-developed octahedral structure (Yang et al., 2017). The first peak assigned to bending vibration of Mn-O-Mn bonding, δ_{Mn-O-Mn} (Nyutu et al., 2008). The two later modes at 581 and 641 cm⁻¹ attributed to stretching bands of the Mn-

O lattice, $\nu_{\text{Mn-O}}$ (Kuo et al., 2015). Fe doping in K-OMS-2 shows broader and lower intensity peaks at about 385, 572, 636 cm^{-1} . Interestingly, after H_2O adsorption, both samples of K-OMS-2 and Fe-OMS-2 show the same vibration bands of prepared Fe-OMS-2. These noticeable peak shift to lower wavenumber of $\delta_{\text{Mn-O-Mn}}$ and $\nu_{\text{Mn-O}}$ may present a lengthening of Mn-O bonding after Fe doping, probably related to enhancement of oxygen vacancies in the structure of cryptomelane. Interestingly, Raman vibration bands of (K-OMS-2 + H_2O) are at the same these of Fe-OMS-2 before and after H_2O adsorption. This suggests deformation of above modes contributed from H_2O adsorbed on nanorod Fe-OMS-2.

Figure 2 shows SEM images of K-OMS-2 and Fe-OMS-2 with nanorod morphology. Diameter of rods is in the range of 30 – 70 nm suggesting nanorod size of cryptomelane prepared from refluxed and coprecipitation methods (Sithambaram et al., 2008). Element analysis from SEM-EDX shows that Fe doping leads an increase of O/Mn molar ratio (Table 1). BET surface area of K-OMS-2 and Fe-OMS-2 are about 170 m^2/g .

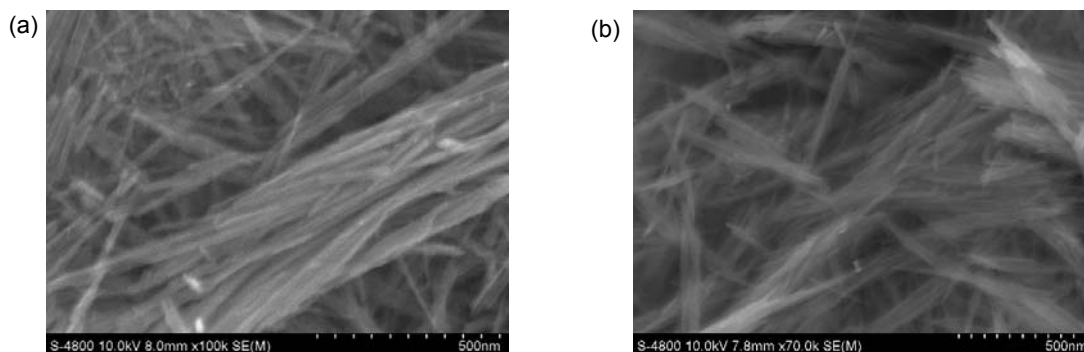


Figure 2: SEM images of (a) K-OMS-2, (b) Fe-OMS-2.

Table 1: Physicochemical properties of samples.

Sample	Element wt%				O/Mn molar ratio	S_{BET} (m^2/g)
	O	K	Mn	Fe		
K-OMS-2	31.7	4.4	63.9	0	0.5	170
Fe-OMS-2	32.4	3.7	54.9	9.0	0.6	168

Figure 3a shows the effect of Fe-OMS-2 concentration ($[\text{Fe-OMS-2}]$) on AB-62 removal yield (amount of AB-62 was decolorized per gram of catalyst) with time. AB-62 removal yield increases with increase of $[\text{Fe-OMS-2}]$ from 0.05 to 0.1 g/L. However, the yield gets a noticeable decrease at further increase of $[\text{Fe-OMS-2}]$ (Figure 3a) indicating that mass transfer control at above 0.1 g/L of $[\text{Fe-OMS-2}]$. Hence, 0.1 g/L of catalyst concentration was chosen for kinetic study in the report. Fe-OMS-2 catalyst was reused for the ozonation of AB-62 indicating the minimal loss of activity up to 4th run (Figure 3b).

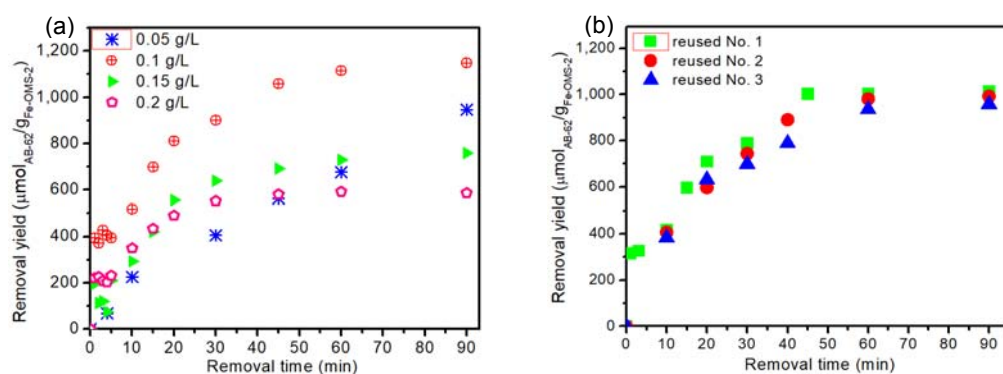


Figure 3: Effect of (a) Fe-OMS-2 concentration on removal yield of AB-62 versus time; (b) Catalyst performance of re-used Fe-OMS-2 with time. Catalytic ozonation conditions are at 27 °C, neutral pH, under 58 $\mu\text{mol}/\text{min}$ of O_3 bubbling.

Figure 4a shows a comparison of catalyst performance of K-OMS-2 and Fe-OMS-2 in the presence and absence of O_3 at RT. There is only about 15 % of AB-62 removal efficiency over Fe-OMS-2 via adsorption in O_2 /air bubbling flow (Fe-OMS-2 + O_2 /air). Ozonation of AB-62 without catalyst shows a linear trend versus time. In the assistance of K-OMS-2, AB-62 removal efficiency is significantly enhanced under O_3 flow (Figure 4a). For instance, only ~40 % of AB-62 was removed after 60 min under non-catalytic ozonation; whereas ~70 % of that was recorded in the presence of K-OMS-2, indicating the ozonation of AB-62 provoked by cryptomelane phase. Noticeably, the removal efficiency over Fe-OMS-2 achieves above 80 % after 60 min suggesting that Fe doping on cryptomelane leads a positive increase of catalyst performance in ozonation of AB-62. This is similar to other reports of metal doping on cryptomelane structure resulting an enhancement of catalyst activity in wet oxidation of phenol (Abecassis-Wolfovich et al., 2005), total oxidation of benzene (Hou et al., 2013) and combustion of methyl ether (Sun et al., 2013) at low temperature; partial oxidation of propanol to acetone (Chen et al., 2001).

Figure 4b shows the model of pseudo first -order reaction with respect to the AB-62 in non-catalytic ozonation and heterogeneous catalytic ozonation over K-OMS-2 and Fe-OMS-2. The slopes of linear lines from this model are -0.03 ± 0.002 ; -0.01 ± 0.001 and $-0.007 \pm 5 \times 10^{-4}$ for Fe-OMS-2; K-OMS-2 and non-catalytic ozonation, getting well with correlation coefficient (R^2) of above 0.97 in kinetic study.

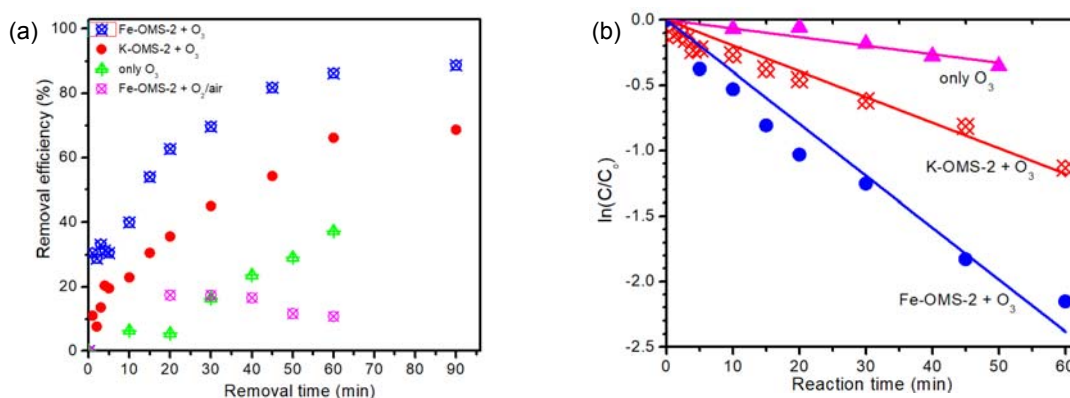


Figure 4: (a) A comparison of catalyst performance in ozonation of AB-62 in different conditions; (b) The pseudo first-order reaction with respect to the AB-62 in non-catalytic and heterogeneous catalytic ozonation over K-OMS-2 and Fe-OMS-2, at 0.1 g/L of catalyst concentration.

3.2 Discussion

It was reported that $\cdot OH$ species is a vital active one for heterogeneous oxidation processes over metal oxides (Zhang et al., 2014), non-metal oxide catalysts (Tran-Thuy et al., 2017), recently heterogeneous catalytic ozonation in removal of bis-phenol A over nano Fe_3O_4 particles (Ahmadi et al., 2016) or degradation of p-nitrophenol on Fe/active carbon (Rodrigues et al., 2017). Other reported that the excess of Fe(III) may react with O_2^- species leading to termination of the chain reaction and thus provoking the hydroxyl radicals (Zhu and Xu 2004). Furthermore, the feeding H_2O suppressed catalyst performance of Fe-OMS in O_3 decomposition that was not observed over Co-OMS-2 (Ma et al., 2017). Many $\cdot OH_{ads}$ provoked at the Fe-Si interface under inhibition process of O_3 decomposition was considered as a crucial step for 4-chloronitrobenzene removal in aqueous solution (Yuan et al., 2018). In this work, Fe-OMS-2 shows clearly the catalytic effect of the prepared materials during the wastewater treatment process (Figure 4). ν_{Mn-O} bands at 581 and 647 cm^{-1} for K-OMS-2 (Figure 1b) assigned for tensile strength effect on Mn-O bonding. Raman spectroscopy of Fe-OMS-2 and (K-OMS-2 + H_2O) samples shows the red peak shift of ν_{Mn-O} bands to 572 and 636 cm^{-1} , comparing to that of K-OMS-2. Consistently, vanadium doping into K-OMS-2 was reported a red peak shift of ν_{Mn-O} at 580 cm^{-1} causing a decrease of Mn oxidation state (Polvarejan et al., 2004). The similar trend of the red shift of Mn-O bonding from 581 cm^{-1} over K-OMS-2 to ~573 cm^{-1} over Fe-OMS-2 and (H_2O + K-OMS-2) is contributed by the similar effect of many $\cdot OH$ groups on as-prepared Fe-OMS-2, consisting to increase of O/Mn molar ratio from 0.5 (K-OMS-2) to 0.6 (Fe-OMS-2) (Table 1). For Fe-OMS-2, the active $\cdot OH$ groups may weaken Mn-O bonds causing a decrease of Mn-O tensile strength and further contributing to enhance catalyst activity. Our results exhibit that AB-62 removal efficiency over nanorod cryptomelane is much higher than that of non-catalytic ozonation. Moreover, a very low AB-62 removal efficiency studied from the adsorption under air bubbling has proved that intrinsic $\cdot OH$ species on Fe-OMS-2 surface seems to be inactive in AB-62 oxidation at RT (Figure 4a). Importantly, under the same condition, only O_3 shows a lower dye removal efficiency than

that combined with catalyst. Consistently, Park et al. reported that the ozonation rate of para-chlorobenzoic acid in the presence of goethite was enhanced, compared to non-catalytic ozonation (Park et al., 2004). Acceleration of ozone decomposition to $\cdot\text{OH}$ was reported in enhancement of oxalic acid degradation over Fe-Cu-MCM-41 (Chen et al., 2017). Similarly, the CoFe_2O_4 prepared by solvothermal route showed a higher catalyst in decolorization of melanoidin (Chen et al., 2017). Thus, a synergistic effect of Fe-OMS-2 catalyst and O_3 on enhancement of AB-62 removal could be associated to weakening Mn-O bonding. In this work, non-catalytic and heterogeneous catalytic ozonation processes obey with model of the pseudo first-order reaction with respect to the AB-62. Reaction rate observed from Fe-OMS-2 is four times faster than that from non-catalytic ozonation confirming that cryptomelane plays an important role in heterogeneous catalytic ozonation of AB-62 at RT, neutral pH. Besides, reaction rate observed from Fe-OMS-2 is three times faster than that from K-OMS-2 supporting lengthening Mn-O bonding on Fe-OMS-2 contributed to synergistic effect of defects/prepared Fe-OMS-2 and O_3 on enhancement of ozonation of AB-62.

4. Conclusions

Nanorod cryptomelane exhibits better heterogeneous catalyst performance than non-catalytic ozonation of AB-62 at RT, neutral pH. Kinetic study shows the pseudo first-order reaction with respect to the AB-62 in non-catalytic and heterogeneous catalytic ozonation. The reaction rate on Fe-OMS-2 is triple faster than that on K-OMS-2 due to tensile strength effect on Mn-O bonding. The synergistic effect of defects/Fe-OMS-2 and O_3 on removal of AB-62 at RT is firstly reported.

Acknowledgments

This research is funded by Ho Chi Minh City University of Technology - VNU-HCM under grant number T-KTHH-2018-101

References

- Ahmadi M., Hasan R.i, Afshin T., Neemat J., Azar M., 2016, A novel catalytic process for degradation of bisphenol A from queous solutions: A synergistic effect of nano- $\text{Fe}_3\text{O}_4@\text{Alg-Fe}$ on $\text{O}_3/\text{H}_2\text{O}_2$, *Process Safety and Environmental Protection*, 104, 413-433.
- Abecassis-Wolfovich M., Jothiramalingam R., Landau M. V., Herskowitz M., Viswanathan B., Varadarajan T. K., 2005, Cerium incorporated ordered manganese oxide OMS-2 materials: Improved catalysts for wet oxidation of phenol compounds, *Applied Catalysis B: Environmental*, 59 (1), 91-98.
- Chen W., Xukai L., Meiqi L., Laisheng L., 2017, Effective catalytic ozonation for oxalic acid degradation with bimetallic Fe-Cu-MCM-41: operation parameters and mechanism, *Journal of Chemical Technology & Biotechnology*, 92, 2862-2930.
- Chen X., Yan-Fei S., Steven L. S., O'Young C. L., 2001, Catalytic Decomposition of 2-Propanol over Different Metal-Cation-Doped OMS-2 Materials, *Journal of Catalysis*, 197, 292-302.
- DeGuzman R. N., Yan-Fei S., Edward J. N., Steven L. S., Chi-Lin O., Steven L., John M. N., 1994, Synthesis and Characterization of Octahedral Molecular Sieves (OMS-2) Having the Hollandite Structure, *Chemistry of Materials*, 6, 815-836.
- Duan N., Steven L S., Chi-Lin O., 1995, Sol-gel synthesis of cryptomelane, an octahedral molecular sieve, *Journal of the Chemical Society, Chemical Communications*, 1367-1368.
- He M., 2018. Coal Chemical Wastewater Treatment Process Based on Computer Simulation Technology, *Chemical Engineering Transactions*, 67, 499-504.
- Hou J., Liangliang L., Yuanzhi L., Mingyang M., Haiqin Lv., Xiujian Z., 2013, Tuning the K^+ Concentration in the Tunnel of OMS-2 Nanorods Leads to a Significant Enhancement of the Catalytic Activity for Benzene Oxidation, *Environmental Science & Technology*, 47, 13730-13736.
- Jia, J., Yang, W., Zhang, P., Zhang J., 2017, Facile synthesis of Fe-modified manganese oxide with high content of oxygen vacancies for efficient airborne ozone destruction, *Applied Catalysis A: General*, 546, 79-86.
- Kuo C.-H., Islam M M., Altug S P., Sourav B., Abdelhamid M El-S., Wenqiao S., Zhu L., Sheng-Yu C., James F R., Jie H., 2015, Robust mesoporous manganese oxide catalysts for water oxidation, *ACS Catalysis*, 5, 1693-1699.
- Ma J., Caixia W., Hong H., 2017, Transition metal doped cryptomelane-type manganese oxide catalysts for ozone decomposition, *Applied Catalysis B: Environmental*, 201, 503-513.
- Martins R.C. and Quinta-Ferreira R. M., 2014, A Review on the Applications of Ozonation for the Treatment of Real Agro-Industrial Wastewaters, *Ozone, Science & Engineering*, 36 (1), 3-35.

- Meyrav A. W., Jothiramalingam R., Landau M. V., Herskowitz M., Viswanathan B., Varadarajan T. K., 2005, Cerium incorporated ordered manganese oxide OMS-2 materials: Improved catalysts for wet oxidation of phenol compounds, *Applied Catalysis B: Environmental*, 59, 91-98.
- Nyutu E. K., Chun-Hu C., Shanthakumar S., Vincent M. B. C. Steven L S., 2008, Systematic control of particle size in rapid open-vessel microwave synthesis of K-OMS-2 nanofibers, *The Journal of Physical Chemistry C*, 112, 6786-6793.
- Oliveira J. S. D., Julia d. S. S., Raquel C. K., Sérgio L. J., Edson L. F., 2019, Catalytic Ozonation of Melanoidin in Aqueous Solution over CoFe₂O₄ Catalyst, *Materials Research*, 22 (1), 1-9.
- Park J.-S., Heechul C., Jaewon C., 2004, Kinetic decomposition of ozone and para-chlorobenzoic acid (pCBA) during catalytic ozonation, *Water research*, 38, 2285-2292.
- Polverejan M., Josanlet C. V., Steven L. S., 2004, Higher Valency Ion Substitution into the Manganese Oxide Framework, *Journal of the American Chemical Society*, 126, 7774-7775.
- Rakness K., Gilbert G., Bruno L., Willy M., Nobuo M., Yves R., C-Michael R., Isao S., 1996, Guideline for measurement of ozone concentration in the process gas from an ozone generator, 18, 209-229.
- Rivera-Utrilla J., Sanchez-Polo M., 2002, Ozonation of 1,3,6-naphthalenetrisulphonic acid catalysed by activated carbon in aqueous phase, *Applied Catalysis B: Environmental*, 39 (4), 319-329.
- Rodrigues C. S. D., Soares O. S. G. P., Pinho M. T., Pereira M. F. R., Luis M. M., 2017, p-Nitrophenol degradation by heterogeneous Fenton's oxidation over activated carbon-based catalysts, *Applied Catalysis B: Environmental*, 219, 109-131.
- Sithambaram S., Edward K. N., Steven L. S., 2008, OMS-2 catalyzed oxidation of tetralin: A comparative study of microwave and conventional heating under open vessel conditions, *Applied Catalysis A: General*, 348, 214-234.
- Sun M., Lin Y., Fei Y., Guiqiang D., Qian Y., Zhifeng H., Yuying Z., Lixiang Y., 2013, Transition metal doped cryptomelane-type manganese oxide for low-temperature catalytic combustion of dimethyl ether, *Chemical Engineering Journal*, 220, 320-347.
- Tran-Thuy T.-M., Chin-Chih C., Lin S. D., 2017, Spectroscopic studies of how moisture enhances CO oxidation over Au/BN at ambient temperature, *ACS Catalysis*, 7, 4304-4316.
- Turhan K., Ozturkcan S. A., 2013, Decolorization and Degradation of Reactive Dye in Aqueous Solution by Ozonation in a Semi-Batch Bubble Column Reactor, *Water, Air, & Soil Pollution*, 224, 1353-1361.
- Valdés H., Rolando F T., Claudio A. Z., 2012, Role of surface hydroxyl groups of acid-treated natural zeolite on the heterogeneous catalytic ozonation of methylene blue contaminated waters, *Chemical engineering journal*, 211, 388-395.
- Villegas J. C, Luis J G., Sinue G., Jason P. D., Steven L S., 2005, Particle size control of cryptomelane nanomaterials by use of H₂O₂ in acidic conditions, *Chemistry of Materials*, 17, 1910-1928.
- Wang J., Jifeng C., Yiren W., Ye W., Hongling Y., Zhi Y., 2018, Odour Treatment Method of Wastewater Treatment Plant Based on Biological Oxidation Process, *Chemical Engineering Transactions*, 68, 457-62.
- Wu J., Huu D., and Simant U., 2008, Decolorization of aqueous textile reactive dye by ozone, *Chemical Engineering Journal*, 142, 156-160.
- Yang J., Hao Z., Lei W., Yexin Z., Chunlin C., Hualei H., Guozheng L., Yajie Z., Yuping M., Jian Z., 2017. Cobalt-Doped K-OMS-2 Nanofibers: A Novel and Efficient Water-Tolerant Catalyst for the Oxidation of Carbon Monoxide, *Chemical Catalysis Catalytical Chemistry*, 9, 1163-1167.
- Yin J., Gaozu L., Jialu Z., Chumei H., Yu L., Ping L., Laisheng L., 2016, High performance of magnetic BiFeO₃ nanoparticle-mediated photocatalytic ozonation for wastewater decontamination, *Separation and Purification Technology*, 168, 134-140.
- Yuan L., Jimin S., Pengwei Y., Zhonglin C., 2018, Interface Mechanisms of Catalytic Ozonation with Amorphous Iron Silicate for Removal of 4-Chloronitrobenzene in Aqueous Solution, *Environmental Science & Technology*, 52, 1429-1434.
- Zhang J., Kyong-Hwan L., Longzhe C., Tae-seop J., 2009, Degradation of methylene blue in aqueous solution by ozone-based processes, *Journal of Industrial and Engineering Chemistry*, 15, 185-189.
- Zhang M., Moreno D. R., Heinz F., 2014, Time-resolved observations of water oxidation intermediates on a cobalt oxide nanoparticle catalyst, *Nature chemistry*, 6, 362-367.
- Zhao D., Liu X., Wang D., Zhou X., Liu Z. Yuan W., 2019, Hydrogenation of acetylenic contaminants over Ni-Based catalyst: Enhanced performance by addition of silver, *Journal of Cleaner Production*, 220, 289-297.
- Zhao L., Zhizhong S., Jun M., 2009, Novel relationship between hydroxyl radical initiation and surface group of ceramic honeycomb supported metals for the catalytic ozonation of nitrobenzene in aqueous solution, *Environmental Science & Technology*, 43, 4157-4163.
- Zhu X.-F., Xu X.-H., 2004, The mechanism of Fe (III)-catalyzed ozonation of phenol, *Journal of Zhejiang University-Science A*, 5(12), 1543-1547.